Available online at www.sciencedirect.com
SCIENCE DIRECT®
Catena 55 (2004) 277–291
CATENA
www.elsevier.com/locate/catena

Genesis of clayey bodies in Quadrilátero Ferrífero, Minas Gerais, Brazil

M.C. Santos[a,b,*], A.F.D.C. Varajão[a], J. Yvon[b]

[a] *DEGEO—Departamento de Geologia, Universidade Federal de Ouro Preto-Campus Universitásio s/n, 35400-000, Ouro Preto, Brazil*

[b] *LEM—Laboratoire Environnement et Minéralurgie/ENSG/INPL, 15 Avenue du Charmois BP 40-54501, Vandoeuvre-les-Nancy, France*

Received 4 September 2002; received in revised form 10 April 2003; accepted 27 May 2003

Abstract

This work deals with macromorphological, mineralogical, micromorphological and geochemical studies in clayey bodies from Quadrilátero Ferrífero in order to define their genesis and formation conditions in this geologic province from Minas Gerais State. Methodologies, based on the description of outcrops and drill cores, using X-ray diffraction (XRD), differential and gravimetric thermal analyses (DTA-TG), scanning electron microscopy (SEM), optical analysis of thin sections and chemical analyses allowed for the definition of two different genetic types of clayey bodies. One type, SET 1, occurs upon saprolitic material from Paleoproterozoic rocks in unconformity contact. It is constituted, from the base to the top, by four facies: nodular, ferruginous kaolinitic, mottled kaolinitic, and massive kaolinitic. The origin of this set is related to the deposition of lateritic materials by gravitational process. The faciological differentiation of this set is related to the syn-depositional process and postdepositional mechanisms of ferruginization and deferruginization. The second type, SET 2, is composed by an ilmenitic–kaolinitic tabular facies in discordant relationships with the saprolite material from Paleoproterozoic rocks. The origin of this second set is related to ''in situ'' alteration of intrusive rocks of acidic composition.

Keywords: Kaolinite; Lateritic profile; Micromorphology; Weathering; Gravity mass flow; Vermelhão mine

* Corresponding author. DEGEO—Departamento de Geologia, Universidade Federal de Ouro Preto-Campus Universitásio s/n, 35400-000, Ouro Preto, Brazil. Tel.: +33-3-83-59-62-66; fax: +33-3-83-59-62-55.
E-mail address: du@degeo.ufop.br (M.C. Santos).

0341-8162/$ - see front matter © 2003 Elsevier B.V. All rights reserved.
doi:10.1016/S0341-8162(03)00106-1

1. Introduction

The Quadrilátero Ferrífero is an important geologic province from Minas Gerais state, Southeast Brazil, that covers an area of nearly 7.000 km^2 (Fig. 1). This region comprises Archean granite–gneisses (metamorphic complex) and two supergroups of supracrustal formations (Dorr, 1969): the Archean Rio das Velhas supergroup and the Paleoproterozoic Minas supergroup with its widespread banded iron formations (BIF). The geomorphic evolution of this region reflects climatic changes (Volkoff, 1985) coupled with tectonic and lithologic control (Varajão, 1991). Three main summital surfaces were differentiated (Varajão, 1991): the highest with altitudes over 1500 m, the intermediate with altitudes ranging from 1100 to 1200 m, and the lowest with altitudes varying from 800 to 900 m. The intermediate and the low surfaces are correlated to two main regional erosional cycles that resulted in the Paleogene Sulamericana and Plio-Pleistocene Velhas surfaces (King, 1957).

The geological structural pattern of the Quadrilátero Ferrífero results from a complex extensional and compressional Transamazonian orogeny in the Paleoproterozoic (Endo and Chemale, 1991; Chemale et al., 1991; Endo, 1997; Alkmim and Marshak, 1998). This tectonism generated synclines and anticlines, such as the Dom Bosco syncline in the southern part of the Quadrilátero Ferrífero (Fig. 1). After the Precambrian deformation, Cenozoic graben zones were generated and filled during periods of reactivation and increased erosion under arid/subarid climate (Santos, 1998; Santos et al., 1999, 2000; Lipski, 2002) as consequence of paleoclimatic evolution throughout the Tertiary and Quaternary (Tardy et al., 1991). Many sediments were formed in these structures and specifically in Dom Bosco syncline, clayey bodies from Vermelhão mine exemplify this regional depositional event. The Vermelhão mine is traditionally known for the exploration of the imperial topaz, and the open mining activities led the exposition of the clayey bodies that are the object of this investigation.

In the stratigraphic context, the Dom Bosco syncline is formed by Paleoproterozoic rocks from the Piracicaba Group, the upper group of the Minas supergroup and by Cenozoic clayey bodies (Dorr, 1969; Johnson, 1962). The Proterozoic rocks include quartzites, phyllites and schists where the main mineralogical paragenesis is muscovite, biotite, quartz, clorite, kyanite, leucoxen, epidote, rutile, tourmaline and zircon. The origins of the clayey bodies are controversial. According to D'Elboux and Ferreira (1975) and Ferreira (1983), they resulted from a simple in situ weathering of volcanic rocks. However, Santos (1998) and Santos et al. (1999, 2000) postulated that these bodies have two distinct origins, one being sedimentary and the other resulting from an in situ weathering of intrusive rocks.

The present study aims at understanding the origin of the clayey bodies of the Quadrilátero Ferrífero and the relationships to formation conditions of the Cenozoic sedimentation in this geologic province. The investigations, based on sedimentological and pedological field observations, were supported by detailed mineralogical, micromorphological and chemical analysis.

2. Materials and methods

The area studied (Vermelhão mine) is located at the Dom Bosco syncline, southern part of Quadrilátero Ferrífero near the town of Ouro Preto (Fig. 1).

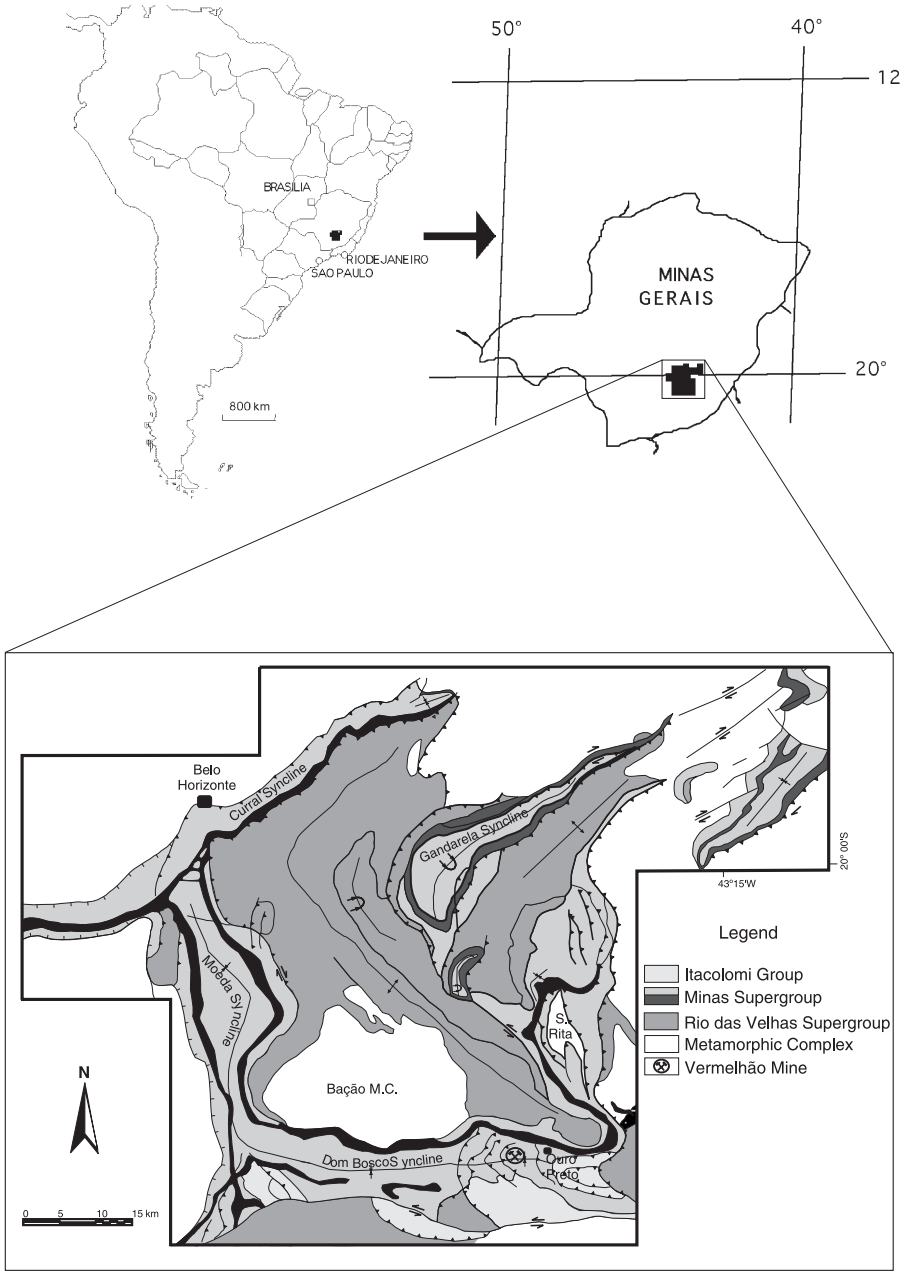

Fig. 1. Location map of the Quadrilátero Ferrífero showing the Dom Bosco Syncline that includes the Vermelhão Mine (modified after Endo, 1997).

The study was initiated by field investigation based on sedimentological description (Graham, 1988) and pedological features (Nahon, 1991; Tardy, 1993) in order to identify the different facies for which 110 samples were collected from the outcrops and from three cores drilled through the entire clayey sequence and the saprolite. Samples were air-dried and Munsell colors (Munsell Soil Color Charts, 1975) were described. Sixty samples were crushed in an agate mortar, ultrasonically dispersed in distilled water, and the clay fraction (< 2 mm) was separated in suspension using a standard sedimentation procedure. X-ray diffraction (XRD) analysis was performed on the whole set of samples and for the clay fraction, on both randomly and parallel oriented samples, by using a Rigaku D/MAX-2B diffractometer with a monochromatic CuKα radiation. Randomly oriented samples were prepared by loading the powder in the aluminium holder with a glass slide at the bottom. Oriented samples were prepared by dropping the clay suspension on the ceramic plates under suction until a thin film was formed. Differential and gravimetric thermal analyses (DTA-TG) were also performed on each sample using an SDT 2960 TA DTA-TGA instrument. Heavy minerals were separated from 16 samples using bromoform, and thin sections were prepared for optical microscope examination. The opaque minerals were examined under reflected polarized light.

Optical microscopic investigations were also carried on 35 thin sections of undisturbed samples using the concepts and terminologies of Brewer (1964, 1976). Morphological aspects of the clay particles were investigated on six samples using a scanning electron microscope (SEM—Jeol JXA-50A) fitted with an energy dispersive X-ray detector (EDX).

Seven whole samples were selected and sent to the Activation Laboratories (ACT-LABS) in Canada for chemical analyses of major, trace and rare-earth elements. The major and trace elements were analyzed using X-ray fluorescence spectroscopy (XRF) and the rare earths using inductively coupled plasma spectrometry (ICP) and instrumental neutron activation analysis (INAA).

3. Results

3.1. Macromorphology, micromorphology and mineralogy

The study of the open mine outcrops and drill cores led to the definition of two types of clayey bodies (Fig. 2). The first type, SET 1, includes four facies from the base to the top: nodular, ferruginous kaolinitic, mottled kaolinitic and massive kaolinitic. All these facies are superposed to the eroded surface of the Piracicaba Group saprolites. The second type, SET 2, is composed of only one facies: the ilmenitic–kaolinitic facies. These bodies have a tabular morphology and show a discordant contact with the rocks of the substrate, the saprolite from the Piracicaba Group. This saprolite comprises intercalations of muscovite–phyllites, carbonous–phyllites and ferruginous–quartzites giving rise to well-defined schistosity.

3.1.1. SET 1

3.1.1.1. Nodular facies. The nodular facies occurs in the lower part and at the border of the deposit in erosive contact with the local basement (Piracicaba Group rocks). It has a

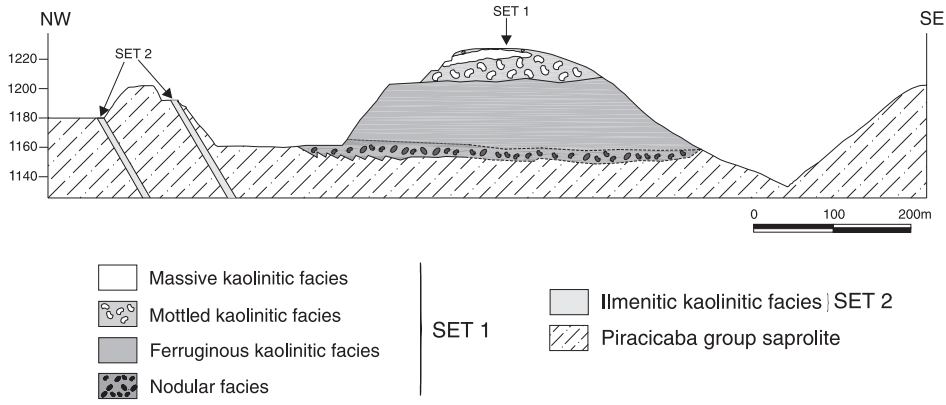

Fig. 2. Schematic cross section of Vermelhão mine showing the distribution of the clayey facies.

thickness ranging from 1.5 to 9 m, and the passage to the ferruginous kaolinitic facies is gradual. These facies consists of lithic fragments and nodules (1 to 2 cm) dispersed in a brown-reddish (5YR 4/4) to yellowish-red (5YR 4/6) clayey matrix with dispersed quartz grains (Fig. 3A).

Microscopic examination reveals the skeleton grains formed mainly by quartz (40%) and muscovite (5%), and secondarily by heavy minerals (1%), such as kyanite, leucoxen, epidote, rutile, tourmaline and zircon, associated to a ferruginous-clay plasma. The paragenesis of heavy minerals is the same as in the Piracicaba Group-one. The silasepic and argillasepic plasmic fabrics are composed of hematite and goethite with kaolinite subordinate. This plasma also contains irregular dark-brown ferruginous stains of goethitic and hematitic composition. Several types of glaebules (Brewer, 1964) are disseminated within the s-matrix in the following forms:

- round-shaped ferruginous glaebules with undifferentiated internal fabric of various sizes (0,016 to 3 mm), black and dark-red, of hematitic and goethitic composition. These pedological features, defined as nodules (Brewer, 1964), have an irregular distribution and present a red and yellow cortex with a sharp external boundary with the plasma. Commonly, there are nodules with broken halos in abrupt contact with the matrix, indicating inherited features (pedorelicts, Fig. 3B).
- glaebules (1–3 mm) including recognizable rock as muscovite quartzite (Fig. 3B), ferruginous quartzite and phyllite with or without dark-red halos. These glaebules are classified as lithorelict nodules (Brewer, 1964).
- glaebules (0.5–2.0 mm) with concentric internal fabric with rather sharp external boundaries related to deferruginization. Brewer (1964) defined these glaebules as concretions.

In this context, the presence of nodules with undifferentiated fabric including recognizable rock (lithorelicts) and soil fabric (pedorelicts), and the erosive contact with the saprolite material from the Piracicaba Group rocks, suggests an allocthonous origin for the nodular facies.

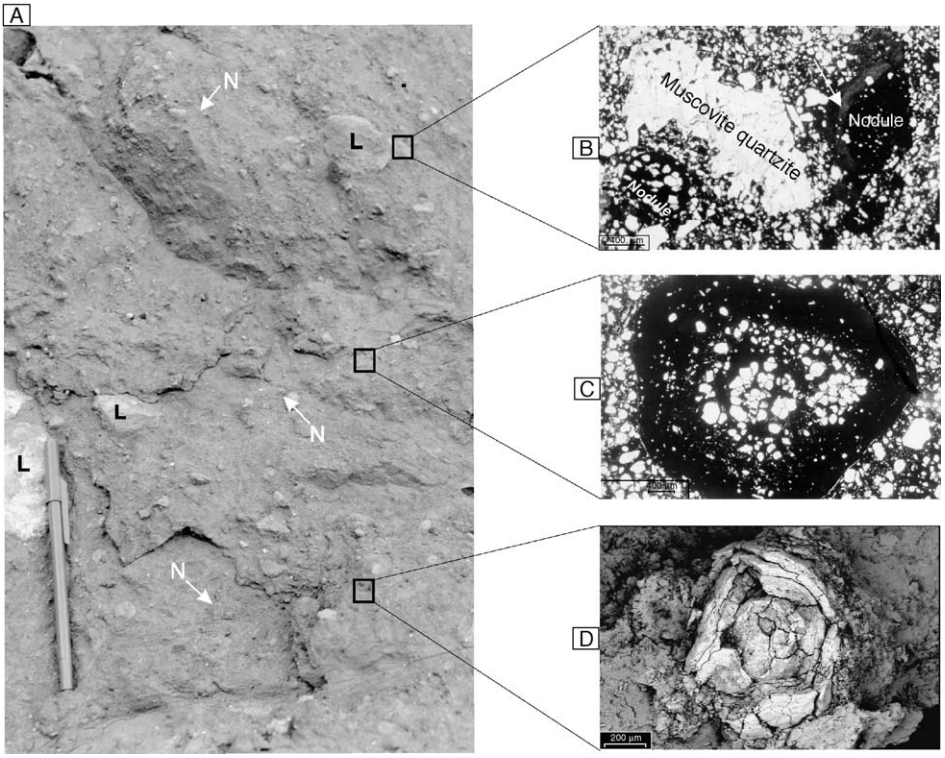

Fig. 3. (A) Sample of the nodular facies showing the lithic fragments (L) and the nodules (N). (B) Optical micrograph (plane polarized light) showing a lithorelict (muscovite quartzite) and pedorelict nodules. Note the broken halos indicated by the arrow. (C) Optical micrograph (plane polarized light) showing nodules including the enclosing s-matrix. (D) SEM micrograph showing a manganese oxide nodule.

Besides the allocthonous nodules, iron and manganese nodules with undifferentiated internal fabric, massive, or including the enclosing s-matrix are also observed (Fig. 3C). They are unsorted (0.064–3 mm) and generally the transition to the plasma is gradual. These nodules can be assumed to be originated in situ by accretion of iron and manganese oxides (Fig. 3D) that were accumulated by diffusion and crystallization in very small pores of the plasma due to favorable local chemical conditions (Boulangé, 1984; Nahon, 1976; Bocquier et al., 1983). Tardy (1993) describes accumulation of iron and manganese by illuviation in clayey pedorelicts and lithorelicts domains analogous to the present study.

Laterally and towards the central part of the clay body, the concentration and sizes of the nodules and concretions decrease, and the nodular facies gradually pass to the ferruginous kaolinitic facies (Fig. 2).

3.1.1.2. Ferruginous kaolinitic facies. The ferruginous kaolinitic facies is about 40 m thick. It is characterized by a reddish-brown (5YR 4/4) massive clay composed of

kaolinite, muscovite, hematite, and goethite with dispersed quartz grains (Fig. 4A). Commonly, it is cut by a network of 5- to 10-cm fractures forming blocks of up to 1-m diameter. The fractures can be filled by ferruginous material giving rise to a massive iron crust (duricrust). Several fractures are surrounded by white stains, characterizing a deferruginization process.

Optical microscopy reveals the skeleton grains composed by quartz (14–25%), muscovite (5%), heavy minerals (1%) such as kyanite, leucoxen, epidote, rutile, tourmaline and zircon, all of them embedded in a dark-brown plasma. This plasma is similar to that of the nodular facies. It has a silasepic plasmic fabric and is composed of hematite, goethite and kaolinite. The DTA-TG analysis shows a peak of kaolinite dehydroxylation at 503 °C and an exothermic peak at 926 °C. Like in the nodular facies, several types of glaebules represented by lithorelict (ferruginous quartzite, muscovite quartzite and phyllite) and pedorelict nodules are present but in smaller proportions (5%) and smaller sizes.

The similarity of the ferruginous kaolinitic facies and nodular facies, in relation to the different kinds of nodules (lithorelicts and pedorelicts), suggests an allochthonous origin and a common source for both the facies.

3.1.1.3. Mottled kaolinitic facies. The mottled kaolinitic facies is 15 m thick and occurs in the top center of the clayey body in gradual contact with the ferruginous kaolinitic facies. Like the ferruginous kaolinitic facies, the mottled kaolinitic facies is characterized by a reddish-yellow (5YR 4/4) massive clay with dispersed quartz grains. A lattice of fractures cuts all of these facies, forming blocks of centimeter to meter sizes. Elongated white stains surround the fracture surfaces. The contact of these stains with the reddish

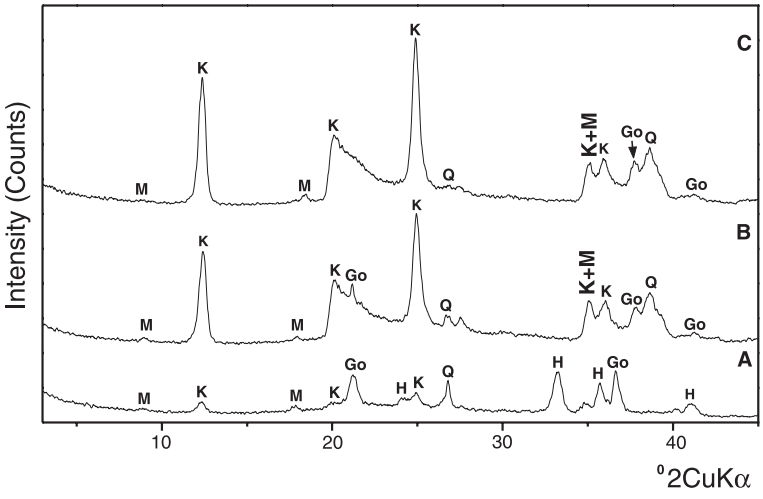

Fig. 4. X-ray diffraction patterns (Cu kα radiation) of randomly oriented samples showing the composition of the (A) reddish-brown clay of the ferruginous kaolinitic facies; (B) white clay of the mottled kaolinitic facies; (C) white clay of the massive kaolinitic facies. K = Kaolinite, M = muscovite, Go = goethite, H = hematite.

clay is gradual passing from white to reddish yellow (5YR 7/6), then yellowish-red (5YR 5/8) and finally reddish-brown (5YR 4/4). These stains become abundant at the top, coalescing to form the whole upper part of the clayey body and characterizing the massive kaolinitic facies.

Microscopically, the s-matrix is mainly formed by quartz skeleton grains (20–25%) and secondarily by particles of muscovite, heavy minerals (2%) analogous to the previous facies and some nodules dispersed in a reddish plasma of kaolinitic–goethitic–hematitic composition, and with a silasepic and argillasepic fabric. The top of the plasma is beige-white with stains (Fig. 5A) of different sizes and different shades of red (dark-red, red, light-red, red-yellowish). These stains have a gradual contact with the beige plasma and contain black to dark-red ferruginous nodules. The diffuse external boundary with the plasma suggests an in situ degradation process due to deferruginization mechanisms from the fracture surfaces.

The XRD patterns from the random powder of the white stains show the dominance of kaolinite with smaller amounts of muscovite, goethite and hematite (Fig. 4B). The absence

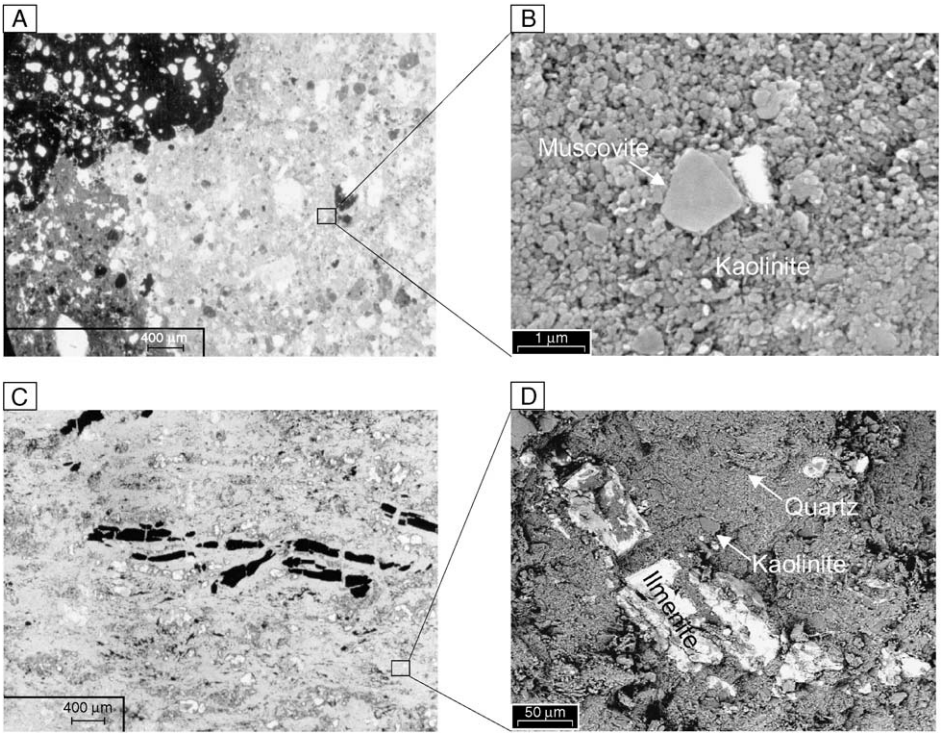

Fig. 5. (A) Optical micrograph (plane polarized light) of the mottled kaolinitic facies showing change color of the stains in the plasma. (B) Scanning electron micrograph of the white stains of the mottled kaolinitic facies showing the small poorly defined crystals of kaolinite surrounding muscovite particle. (C) Optical micrograph (plane polarized light) of the ilmenitic kaolinitic facies showing orientation of the elongated ilmenite. (D) SEM showing the larger crystals of kaolinite in the ilmenitic kaolinitic facies.

of discrete reflections in the [1$\bar{1}$0] (20.4° 2θ CuKα) and [11$\bar{1}$] (21.3° 2θ CuKα) band, used to calculate the Hinckley index (Hinckley, 1963), and the peak temperature of kaolinite dehydroxylation close to 510 °C show a poor crystallinity or small size of the kaolinite crystals (Mackenzie, 1957; Grim, 1968; Brindley and Brown, 1980). These results are consistent with SEM analyses of the white stains showing very poorly defined and small kaolinite crystals typical of pedogenic origin (Varajão et al., 2001; Singh and Gilkes, 1992), together with some particles of muscovite (Fig. 5B).

The similar mineralogical composition of the skeleton grains of these facies and the ferruginous kaolinitic facies, as well as the analogous pedogenic features, indicate a common origin for both. The presence of red stains, including ferruginous nodules, in gradual transition with the white kaolinitic plasma characterizes a deferruginization process that led to the change of the ferruginous facies to the mottled kaolinitic facies.

3.1.1.4. Massive kaolinitic facies. The massive kaolinitic facies occur at the upper central part of the deposit in gradual contact with the mottled kaolinitic facies. Macroscopically, it is characterized by white clay with local, irregular, centimeter-sized reddish stains and with dispersed quartz grains.

Optical microscopy showed the same micromorphological features as those from the previous facies: an s-matrix constituted by dispersed quartz skeleton (25%) and traces of muscovite embedded in a kaolinitic plasma. The heavy mineral paragenesis is also similar to that of the mottled kaolinitic facies and represents less than 2% of the s-matrix. Locally, one can observe irregular, small, reddish stains related to degraded ferruginous nodules, embedded in the plasma.

Like for the mottled kaolinitic facies, XRD patterns from the random powder of the white clay show the dominance of kaolinite with smaller amounts of muscovite and goethite (Fig. 4C). Here also, the absence of discrete reflections at the range of 20–24° 2θ indicates a low crystallinity of the kaolinite crystals (Brindley and Brown, 1980). DTA-GT analysis also corroborates these results showing a peak temperature of kaolinite dehydroxylation of 509 °C, which is characteristic of poor order or small size of the kaolinite crystals (Mackenzie, 1957; Grim, 1968). Identically, the SEM analysis of the white clay shows small crystals of kaolinite suggesting a pedogenic origin (Varajão et al., 2001; Singh and Gilkes, 1992).

The similar mineralogical association of the skeleton grains, together with the analogous micromorphological and pedogenic features, suggests that all the facies from SET 1 have a common source area. The absence of orientation of the skeleton grains, the presence of lithic fragments and heterogeneous nodules and the erosive contact of the basal facies (nodular facies) indicate an allochthonous origin associated with gravitational transport.

3.1.2. SET 2

3.1.2.1. Ilmenitic kaolinitic facies. These facies was observed in the outcrops in the northwestern part of the mine (Fig. 2) and at a depth of 84.0 m in one core drill, intercalated in the saprolite. It has a thickness ranging from 4 to 12 m and occurs in discordant contact with the Piracicaba Group saprolites (phyllites and ferruginous quartz-

ites). It is characterized by a white to light pink (5YR 8/3) clay enveloping elongated crystals of oriented and broken ilmenite and quartz grains.

Optical microscopy shows a banded feature characterized by the intercalation of layers of quartz (10–25%) and layers of ilmenite (5%), both of them surrounded by a kaolinitic plasma with a silasepic fabric. The ilmenite crystals are elongated and oriented towards the same direction with fractures perpendicular to the direction of crystal growth (Fig. 5C). The quartz is stretched parallel to the ilmenite crystals. The paragenesis of the heavy minerals (< 3%) is represented only by martite, magnetite, and zircon, different from the facies of SET 1: kyanite, leucoxen, epidote, rutile, tourmaline and zircon. The paragenesis from the SET 1 is the same as that of the saprolite basement.

Table 1
Major (wt.%), trace and REE (ppm) elements in the samples from the SET 1, SET 2 and Piracicaba Group saprolite

Facies	Massive kaolinitic	Mottled kaolinitic	Ferruginous kaolinitic	Nodular	Ilmenitic kaolinitic	Phyllite	Quartzite
(wt.%)							
SiO_2	45.24	44.74	22.54	53.18	50.00	27.94	68.96
Fe_2O_3	1.73	1.51	43.21	23.76	7.77	40.18	6.49
Al_2O_3	34.67	34.16	15.11	12.34	25.37	10.35	6.79
TiO_2	2.27	4.09	2.10	1.88	4.21	1.33	2.65
Total	83.84	84.50	82.96	91.16	87.35	79.80	94.89
(ppm)							
As		4.6	24	31	< 0.5	49	5.9
Ba	230	250	620	1600	250	5800	3500
Co	2	1	5	7	4	9	71
Cr	66	120	130	76	62	130	79
Cs	2	< 2	< 1	2	< 1	2	2
Cu	28	34	64	61	35	34	93
Hf	13	15	6	5	10	2	5
Mn	49	58	3906	4180	767	22 991	513
Rb	21	< 15	< 15	39	< 15	63	90
Sb	20	7.4	2.8	3.6	1.3	4.5	2.0
Sc	17	43	18	14	27	18	17
Ta	2.6	3.1	1.2	1.3	< 0.5	1.2	1.1
Th	29	32	14	9.5	10	12	9.3
U	4	5.0	6.3	3.5	< 0.5	3.3	3.92
V	34	55	134	85	175	22	160
Y	22	28	14	13	34	74	16
W	5	< 1	3	< 1	< 1	6	< 1
La	52	82	14	21	220	44	26
Ce	120	160	30	41	280	55	47
Nd	30	54	8	< 5	180	41	22
Sm	10	9.3	1.8	1.9	28	7.9	4.7
Eu	3.7	1.9	0.5	0.6	7.2	2.3	1.2
Tb	2.2	< 0.5	< 0.5	< 0.5	2.4	1.4	< 0.5
Yb	4.1	4.7	2.2	2.2	2.8	8.7	2.3
Lu	0.64	0.70	0.37	0.38	0.54	1.41	0.36
Total	313.1	226.6	57.4	72.6	720	161.7	104.1

The XRD patterns of the clay show the dominance of quartz and kaolinite with traces of hematite and goethite. Similarly to SET 1, the absence of discrete reflections at the range of 20–24 ° 2θ and a peak temperature of dehydroxylation of 505 °C suggest poorly ordered kaolinite crystals. The SEM analysis showed crystal flakes of kaolinite of irregular shapes but of larger sizes than in SET 1.

3.2. Chemical composition

Chemical analyses were made for all the facies of SET 1, SET 2 and on two samples of the Piracicaba Group saprolite (phyllite and quartzite) (Table 1). The superficial facies of SET 1 (mottled kaolinitic and massive kaolinitic facies) are relatively richer in Al_2O_3 while the lower facies (nodular and ferruginous kaolinitic facies) are richer in Fe_2O_3. This differentiation is related directly to the deferruginization that occurs in the upper facies from the SET 1, corroborating the micromorphological study. Among the trace elements, Ba and Cr can be singularized, presenting an elevated concentration in the bottom facies of SET 1. This concentration is also high in the Piracicaba Group saprolite rocks, suggesting a strong contribution of these rocks to the facies mentioned above. The anomalous content of Mn in these facies can be attributed to postdepositional supergenic processes. The source of this element is the local basement, especially the phyllites.

The standard distribution of the rare-earth elements (REE), chondrite-normalised (Fig. 6), shows an increase in light rare earth (LREE) and depletion of heavy rare-earth elements

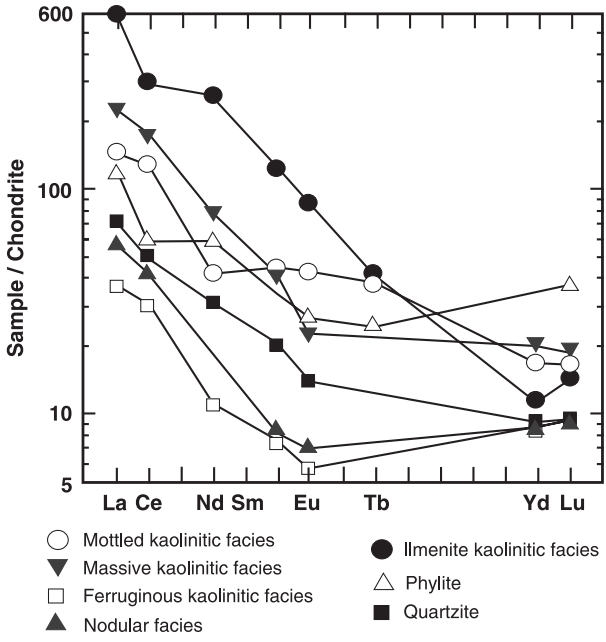

Fig. 6. Distribution of REE in samples from the facies of SET 1, SET 2 and saprolite, chondrite normalized.

(HREE). The rate $(La/Yb)_N$ for the facies from SET 1 are between 4.2 and 11.25 (Table 1). The bottom facies are richer in HREE and the upper facies are poorer in these elements. SET 2 shows a rate $(La/Yb)_N$ of 50 and consequently a strong depletion in HREE. For the samples of the Piracicaba Group saprolite (phyllites and quartzites), the rate $(La/Yb)_N$ is 3.42 and 7.0, showing an elevated concentration of HREE analogously to the lower facies from the SET 1. When comparing the REE distribution graph of the facies from the bottom of SET 1 with the rocks of the local basement saprolite (Fig. 6), a great similarity is noted, suggesting that the nodular and ferruginous kaolinitic facies both received a strong contribution of sediments from the local basement, via the Piracicaba Group saprolite. The upper facies present this contribution too. However, they have some similarity with the ilmenitic–kaolinitic facies (SET 2), such as the elevated concentration of LREE and, particularly, the absence of depletion in Eu in the mottled kaolinitic facies. This fact suggests a contribution of sediments from the SET 2 in the upper facies from the SET 1. However, the anomalous La concentration in the standard distribution REE of SET 2 makes the differentiation between these facies and the upper facies from SET 1. The graph from the SET 2 is very similar to the REE standard distribution of silica-supersaturated intrusive rocks, as the example of the batholith of Itiúba in Brazil (Figueredo, 1981).

4. Discussion and conclusion

The studies performed on the clayey bodies from the Vermelhão Mine led to the characterization of two sets: SET 1 of sedimentary origin and SET 2 of intrusive origin.

The SET 1 was generated from the deposition of clayey sediments in small grabens formed in the Dom Bosco syncline during the Tertiary (Santos, 1998, Santos et al., 1999, 2000; Lipski, 2002). The sediments were deposited by gravitational processes due to the influence of heavy storms associated to subarid conditions in the Pliocene (Maizatto, 1997). As the sediments are clayey, with subordinate portions of lithic fragments and pedogenic nodules, this association indicates that the source area was a thick regolith formed under humid climate (Miocene) from the alteration of the rocks of the Piracicaba Group, local basement. The climate changes in the Quadrilátero Ferrífero were proposed by Maizatto (1997) from palynological records in the sediments. In the global context, Parrish et al. (1982) and Tardy et al. (1991) described climate variations in the Miocene–Pliocene and their influence in the formation of laterites in Africa and Brazil.

It is traditionally known that in the intertropical regions, the weathered mantle is thick and chemically highly evolved with the formation of laterites. According to Tardy (1969), Tardy and Nahon (1985) and Nahon (1986), a typical and well-preserved lateritic profile comprises a vertical succession of horizons constituted, from the base to the top, by a coarse saprolite, fine saprolite, mottled clay zone and nodular horizons with Fe and Al accumulation.

The features described in the nodular facies showing fragmented nodules, nodules with recognizable rock fabric (lithorelicts) and soil fabric (pedorelicts) suggest that these facies was originated from the regolith materials already available in the source area, in the

lateritic profile higher in the landscape. Similar event has been described by Millot (1964) that shows the mechanical erosion action on the iron crusts along the valley sides and the formation of pediments with lateritic gravels. In the present study, the differentiation of facies of the SET1 is characterized by an inverse lateritic profile, where the nodular facies that occurs at the bottom of the clayey body is related to the nodular horizon of the lateritic profile. The ferruginous kaolinitic facies that occurs in the middle of the deposit is related to the mottled clay zone of the lateritic profile. The mottled kaolinitic and massive kaolinitic facies also present the contribution of the mottled clay zone of the lateritic profile. However, the elevated concentration of LREE and the absence of depletion in Eu, shown in their REE distribution, make some differentiation between them and the nodular and ferruginous kaolinitic facies, with respect to the source material. For the upper facies (mottled kaolinitic and massive kaolinitic facies), a mix with the materials of the SET 2 suggests that the clayey body of the SET 2 was also located in higher landscape units and could therefore supply sediments to the basin.

After the deposition of SET 1, iron and manganese illuviation originated from the saprolite in the adjoining slopes was responsible for the formation of the nodules with the fabric of the enclosing s-matrix. These nodules show an in situ accretion of Mn and Fe that accumulated in the s-matrix due to favorable local chemical conditions. The iron transfers via solutions in the intergranular porosity can induce the nucleation and growth of hematite, hematite–goethite and goethite particles (Boudeulle and Muller, 1988). According Nahon (1976), Bocquier et al. (1983) and Tardy (1993), the iron remobilization or mass transfer can be related to the unsaturated domain, seasonally hydrated and dried.

For SET 2, the discordant contact with the Piracicaba Group saprolite, as well as the distinct paragenesis, the larger sizes of the kaolinite crystals and the structural features compared to the facies from SET 1, indicate a different origin for these facies. The high concentration of quartz grains associated with the ilmenite–magnetite paragenesis and the high content of LREE suggest that these facies was originated from in situ weathering of acidic intrusive rock. The orientation of the ilmenite and quartz may have been originated during a magmatic re-mobilization or deformation. The fact that the crystals of the ilmenite have fractures perpendicular to their elongation may be possibly related to a micro pull-apart, brittle deformation.

Micromorphological features associated to the chemical data were shown to be fundamental to the differentiation of the clayey bodies and to provide a basis for interpretations of temporal relationships, potentially useful to unravel the geological history in highly weathered terrains. The type of sedimentation and nature of the facies that reflected the global climatic changes elucidates the nature of Cenozoic sedimentation in the Quadrilátero Ferrífero.

Acknowledgements

The authors acknowledges CAPES/COFECUB, CNPq and FAPEMIG for their financial support, and the Vermelhão mine for providing the samples. The authors are grateful to the two reviewers, Y. Tardy and G. Stoops, for their constructive criticisms of the manuscript.

References

Alkmim, F.F., Marshak, S., 1998. Transamazonian Orogeny in the Southern São Francisco Craton region, Minas Gerais, Brazil: evidence for Paleoproterozoic collision and collapse in the Quadrilátero Ferrífero. Precambrian Research 90, 29–58.

Bocquier, C., Boulangé, B., Ildefonse, P., Nahon, D., Muller, D., 1983. Transfers, accumulation modes, mineralogical transformations and complexity of historical development. In: Melfi, A.J., Carvalho, A. (Eds.), Laterisation Processes. USP, São Paulo, pp. 331–337.

Boudeulle, M., Muller, J.-P., 1988. Structural characteristics of hematite and goethite and relations with kaolinite in laterite from Cameron. ATEM study. Bulletin de MineÂralogie 11, 149–166.

Boulangé, B., 1984. Les formations bauxitiques latéritiques de Côte dIvoire. Les faciès, leur transformation, leur distribution et lévolution du modelé. Trav. et Docum., vol. 175. Service des Publications ORSTOM, Bondy. 363 pp.

Brewer, R., 1964. Fabric and Mineral of Soils. Wiley, New York. 470 pp.

Brewer, R., 1976. Fabric and Mineral of Soils. Reprinted from the edition published by Wiley, New York. Robert E. Krieger Publishing Co., New York. 481 pp.

Brindley, G.W., Brown, G., 1980. Crystal Structures of Clay Minerals and their Identification. Mineralogical Society, London. 495 pp.

Chemale Jr., F., Rosière, C.A., Endo, I., 1991. Evolução tectônica do Quadrilátero Ferrífero-Um modelo. Pesquisas 18 (2), 104–127.

D'Elboux, C.V., Ferreira, C.M., 1975. Topázio na região de Ouro Preto. Boletim do Departamento de Geologia. UFOP. Publicação Especial 1, 73–79.

Dorr, J.V.N., 1969. Physiografic, stratigraphic and structural development of the Quadrilátero Ferrífero, Minas Gerais, Brazil. U.S. Geological Survey Professional Paper, 1–58 (Washington).

Endo, I., 1997. Regimes Tectônicos do Arqueano e Proterozóico no interior da Placa Sanfranciscana: Quadrilátero Ferrrífero e Áreas Adjacentes, Minas Gerais-São Paulo. PhD Thesis, USP, São Paulo, Brazil.

Endo, I., Chemale Jr., F., 1991. Implicações tectônicas das estruturas extensionais no Quadrilátero Ferrífero, MG. Anais 3° Simpósio Nacional de Estudos Tectônicos. SBG, São Paulo, pp. 51–53.

Ferreira, C.M., 1983. Vulcanismo ácido no Quadrilátero Ferrífero e sua relação com algumas ocorrências minerais. Anais 3° Simpósio de Geologia de Minas Gerais, vol. 3. SBG, Belo Horizonte, Boletim, pp. 128–133.

Figueredo, M.C.H., 1981. Geoquímica de rochas metamórficas de alto grau do nordeste da Bahia, Brasil. CPM-SME/BA, Geologia e Recursos Minerais do Estado da Bahia, Boletim 4, 41–71.

Graham, J., 1988. Collection and analysis of field data. In: Tucker, M. (Ed.), Techniques in Sedimentology. Blackwell, Oxford, pp. 5–62.

Grim, R.E., 1968. Clay Minerals, 2nd ed. McGraw-Hill, New York. 596 pp.

Hinckley, D.N., 1963. Variability in "crystallinity" values among the kaolin deposits of Georgia and South Carolina. Clays and Clay Minerals 2, 229–235.

Johnson, R.F., 1962. Geology and ore deposits of the Cachoeira do Campo, Dom Bosco and Ouro Branco Quadrangles, Minas Gerais, Brazil. U.S. Geological Survey Professional Paper (Washington, 37 pp.).

King, L.C., 1957. A geomorfologia do Brasil Oriental. Revista Brasileira de Geografia 18, 147–263.

Lipski, M., 2002. Tectonismo Cenozóico no Quadrilátero Ferrífero, Minas Gerais. Master dissertation DEGEO/EM/UFOP, Ouro Preto.

Mackenzie, R.C., 1957. The Differential Thermal Investigation of Clays. Mineralogical Society, London. 456 pp.

Maizatto, J.R., 1997. Análise paleoecológica bioestratigráfica dos sedimentos cenozóicos da bacia do Gandarela, Quadrilátero Ferrífero, Minas Gerais, com base nos aspectos palinológicos e sedimentares. Master dissertation DEGEO/EM/UFOP, Ouro Preto.

Millot, G., 1964. Géologie des argiles altérations sédimentologie géochimie. Masson & Cie, Paris, pp. 105–162.

Munsell Soil Color Charts, 1975. Macbeth Division of Kollmorgen, Baltimore.

Nahon, D., 1976. Cuirasses ferrugineuses et encroûtements calcaires au Sénégal occidental et en Mauritanie. Systèmes évolutifs: géochimie, structures, relais et coexistence. PhD Thesis, Sci. Marseille III et Sci. Géol. 44.

Nahon, D., 1986. Evolution of iron crusts in tropical landscapes. In: Coleman, S.H., Dethier, D.P. (Eds.), Rates of Chemical Weathering of Rocks and Minerals. Academic Press Inc., San Diego. ch. 9.

Nahon, D., 1991. Introduction to the Petrology of Soils and Chemical Weathering. John Wiley & Sons Inc., New York. 313 pp.

Parrish, J.T., Ziegler, A.M., Scotese, C.R., 1982. Rainfall patterns and the distribution of coals and evaporites in the mesozoic and cenozoic. Palaeogeography, Palaeontology, Palaeoecology 40, 67–101.

Santos, M.C., 1998. Gênese dos Corpos Argilosos do Morro do Caxambu e da Mina do Vemelhão, Sinclinal Dom Bosco, Quadrilátero Ferrífero, Minas Gerais, Brasil. Master dissertation DEGEO/EM/UFOP, Ouro Preto.

Santos, M.C., Varajão, A.F.D., Castro, P.T.A, Moreira, A.P.A., 1999. Gênese dos "depósitos argilosos" da Mina do Vermelhão e do Morro do Caxambu, Sinclinal Dom Bosco, M.G. SBG/Núcleo Brasília. Simpósio de Geologia do Centro-Oeste e Simpósio de Geologia de Minas Gerais.

Santos, M.C., Varajão, A.F.D.C., Castro, P.T.A.C., Moreira, A.P.A., 2000. Sistemas deposicionales de mudstones del sinclinal "Dom Bosco" (Mina do Vermelhào y Morro do Caxambu), Quadrilátero Ferrífero-MG Brasil. 2° Cong. Latinoamericano de Sedimentología, 8^{0} Reunión Argentina de Sedimentología. IAS, Buenos Aires, 162–163.

Singh, B., Gilkes, R.J., 1992. Properties of soil kaolinites from south-western Australia. Journal of Soil Science 43, 645–647.

Tardy, Y., 1969. Géochimie des altérations. Étude des arènes et des eaux de quelques massif cristallins d'Europe et d'Afrique. Mémoire Sérvice Carte Géologique, Alsace, 31.

Tardy, Y., 1993. Pétrologie des Laterites et des Sols L'alteration Initiations. Masson, Paris.

Tardy, Y., Nahon, D., 1985. Geochemistry of laterites, stability of Al–goethite, Al–Hemathite and Fe^{3+}–kaolinite in bauxites and ferricretes: an approach to the mechanism of concretion formation. American Journal of Science 285, 865–903.

Tardy, Y., Kobilsek, B., Paquet, H., 1991. Mineralogical composition and geographical distribution of African and Brazilian periatlantic laterites. The influence of continental drift and tropical paleoclimates during the past 150 million years and implications for India and Australia. Journal of African Earth Sciences 12, 283–295.

Varajão, C.A.C., 1991. A questão da ocorrência das superfícies de erosão do Quadrilátero Ferrífero, Minas Gerais. Revista Brasileira de Geociências 21, 131–145.

Varajão, A.F.D.C., Gilkes, R.J., Hart, R.D., 2001. The relationships between kaolinite crystal properties and the origin of materials for a Brazilian kaolin deposit. Clays and Clay Minerals 49, 44–59.

Volkoff, B., 1985. Organizations regionales de la couverture pédologique du Brésil, Chronologie des differentiations. Cahiers - ORSTOM. Série Pédologie 21, 225–236.